



Search within Journal... 

Issue  Journal




## Volume 41 (2020): Issue 1 (Feb 2020)

in [IAWA Journal](#)

Online ISSN: 2294-1932

Print ISSN: 0928-1541


Publisher: Brill

Subjects 

## Editorial

[The start of a new era](#)

Pages: 1

 15%

What is your opinion of this page?

[Continue](#)

We use cookies to ensure the functionality of our website, to personalize content, to provide social media features, and to analyze our traffic. You can decide for yourself which categories you want to deny or allow. Please note that based on your settings not all functionalities of the site are available. Further information can be found in our [privacy policy](#). [Privacy Statement](#)

### [Cookies Settings](#)

[Accept All Cookies](#)

Pages: 2–11

Online Publication Date: 26 Feb 2020

Micro-CT measurements of within-ring variability in longitudinal hydraulic pathways in Norway spruce

Authors: Robin Adey-Johnson, J. Paul Mclean, Jan Van den Bulcke, Joris Van Acker, and Peter J. McDonald

Pages: 12–29

Online Publication Date: 26 Feb 2020

Wood anatomy of *Ceiba speciosa* (A. St.-Hil.) Ravenna under urban pollution

Authors: Thaís Jorge de Vasconcellos and Cátia Henriques Callado

Pages: 30–47

Online Publication Date: 26 Feb 2020

Cross-field pitting characteristics of compression, lateral, and opposite wood in the *Pinus densiflora*

Authors: Byantara Darsan Purusatama and Nam Hun Kim

Pages: 48–60

Online Publication Date: 26 Feb 2020

Direct exposure to solar radiation causes radial growth eccentricity at the beginning of the growing season in *Robinia pseudoacacia*

Authors: Adam Miodek, Aldona Gizińska, Marcin Klisz, Tomasz Wojda, Krzysztof Ukalski, and Paweł Kojs

Pages: 61–84

Online Publication Date: 26 Feb 2020

Burl formation in mango (*Mangifera indica*): a neglected tumour disorder and the structure of its secondary xylem

Authors: Parmeshwar L. Saran, Ravi S. Patel, Ram P. Meena, Riddhi P. Vasara, and Kishore S. Rajput

Pages: 85–97

Online Publication Date: 26 Feb 2020

Gum duct formation mediated by various concentrations of ethephon and methyl jasmonate treatments in *Cerasus × yedoensis*, *Prunus mume* and *Liquidambar styraciflua*

Authors: Anne Carolina and Dai Kusumoto



15%

What is your opinion of this page?

Continue

We use cookies to ensure the functionality of our website, to personalize content, to provide social media features, and to analyze our traffic. You can decide for yourself which categories you want to deny or allow. Please note that based on your settings not all functionalities of the site are available. Further information can be found in our privacy policy. [Privacy Statement](#)

[Cookies Settings](#)

Accept All Cookies

Pages: 109–124

Online Publication Date: 26 Feb 2020

## Obituary

[Fritz Hans Schweingruber \(1936-2020\)](#)

Dendroecologist and plant anatomist who taught us how to understand plants

Pages: 125–127

Online Publication Date: 26 Feb 2020

## Acknowledgement

[Acknowledgement of Reviewers](#)

Pages: 128–130

Online Publication Date: 26 Feb 2020



15%

What is your opinion of this page?

Continue

### Products

Books

Journals

Reference Works

Primary source collections

COVID-19 Collection

### Services

Authors

How to publish with Brill

Trade

We use cookies to ensure the functionality of our website, to personalize content, to provide social media features, and to analyze our traffic. You can decide for yourself which categories you want to deny or allow. Please note that based on your settings not all functionalities of the site are available. Further information can be found in our privacy policy. [Privacy Statement](#)

### [Cookies Settings](#)

Accept All Cookies

[Open Access and Research Funding](#)

[Open Access for Librarians](#)

[Open Access for Academic Societies](#)

[Open Access Content](#)

### Contact & Info

[About us](#)

[Contact us](#)

[Sales contacts](#)

[Publishing contacts](#)

[FAQ](#)

### Stay Updated

[Blog](#)

[Newsletters](#)

[News](#)

[Catalogs](#)

[Social Media Overview](#)



[Terms and Conditions](#)

[Privacy Statement](#)

[Cookies Settings](#)

[Accessibility](#)

15%

What is your opinion of this page?

Continue

Copyright © 2016-2021

Powered by PubFactory

We use cookies to ensure the functionality of our website, to personalize content, to provide social media features, and to analyze our traffic. You can decide for yourself which categories you want to deny or allow. Please note that based on your settings not all functionalities of the site are available. Further information can be found in our privacy policy. [Privacy Statement](#)

### [Cookies Settings](#)

Accept All Cookies



BRILL

## The occurrence and structure of radial sieve tubes in the secondary xylem of *Aquilaria* and *Gyrinops*

Bei Luo<sup>1,\*</sup>, Tomoya Imai<sup>2</sup>, Junji Sugiyama<sup>2</sup>, Sri Nugroho Marsoem<sup>3</sup>, Tri Mulyaningsih<sup>4</sup>, and Takao Itoh<sup>5</sup>

<sup>1</sup>Southwest Forestry University, Kunming, P.R. China

<sup>2</sup>Kyoto University, Kyoto, Japan

<sup>3</sup>University Gadjah Mada, Yogyakarta, Indonesia

<sup>4</sup>University Mataram, Mataram, Indonesia

<sup>5</sup>Nara National Research Institute for Cultural Properties, Nara, Japan

\*Corresponding author; email: beiluoswfu@qq.com

Accepted for publication: 18 July 2019

### ABSTRACT

New observations of radial sieve tubes in the secondary xylem of two genera and four species of agarwood — *Aquilaria sinensis*, *A. crasna*, *A. malaccensis* and *Gyrinops versteeghii* (Thymelaeaceae) — are presented in this study. The earliest radial sieve tubes in *Gyrinops* are formed in the secondary xylem adjacent to the pith. The radial sieve tubes originate from the vascular cambium and develop in both uniseriate and multiseriate ray tissue. In addition to sieve plates in lateral and end walls, scattered or clustered minute sieve pores are localized in the lateral wall of radial sieve tubes. There is a direct connection between radial sieve tubes in ray tissue and axial sieve tubes in interxylary phloem strands (IP), such as (i) connection by bending of radial sieve tube strands, (ii) connection of two IP strands by an oblique bridge, and (iii) connection of two IP strands at a right angle. The average number of radial sieve tubes and interxylary phloem was found to be 1.7 per mm<sup>3</sup> and 9.1 per mm<sup>2</sup> in the secondary xylem. Considering the higher frequency of radial sieve tubes with the increasing thickness of the secondary xylem, the direct connections between radial and axial sieve tubes could play a significant role in assisting the translocation of metabolites in *Aquilaria* and *Gyrinops*.

**Keywords:** sieve plate; sieve pore; interxylary phloem; agarwood; callose; FE-SEM.

### INTRODUCTION

The vascular cambium forms the secondary vascular tissues, secondary phloem and secondary xylem (Evert 2006; Angyalossy *et al.* 2016). The majority of tree species produce

only one kind of phloem outside the vascular cambium, that is, secondary (or external) phloem, which is predominantly involved in the translocation of photosynthetic products. However, many species belonging to several families, including many lineages of lianas, produce interxylary phloem in addition to the regular secondary phloem (Chalk & Chatterway 1973; van Veenendaal & den Outer 1993; den Outer & van Veenendaal 1995; Carlquist 2002, 2010, 2013; Patil & Rajput 2008; Rajput *et al.* 2009, 2013; Mohamed *et al.* 2011; Patil *et al.* 2011; Angyalossy *et al.* 2012, 2016). Recently, it was suggested that a third type of phloem, the intraxylary phloem, could play a predominant role in translocating reserve food or photosynthetic products, especially before the differentiation of interxylary phloem (IP) in young shoots (Luo *et al.* 2019). Commonly in *Aquilaria* and *Gyrinops*, IP strands are isolated from each other and embedded in the secondary xylem as scattered islands. Even in the vertical direction, the termination of the IP strands do not connect to the other IP strands. So far, it was not known as to how a sieve tube in an isolated IP strand could translocate photosynthates to other IP strands. One possibility being the presence of ray parenchyma tissue passing through the discrete phloem islands in secondary xylem. Recently, Pfautsch *et al.* (2015) suggested that functional links between xylem and phloem transport can be facilitated by radially aligned and interconnected ray parenchyma tissue. Whether this suggestion is applicable to species that produce IP for facilitating the translocation of photosynthates is here elucidated.

Radial sieve tube elements have been reported in different genera and these have been grouped into at least three categories depending on the mechanism by which they are formed. The three categories are (1) naturally developed radial sieve elements in secondary phloem (Chavan *et al.* 1983; Rajput & Rao 1997; Rajput 2004; Angyalossy *et al.* 2012), (2) naturally developed radial sieve elements in secondary xylem (Den Outer & Veenendaal 1981; Lev-Yadun & Aloni 1991; Angyalossy *et al.* 2012; Gondaliya & Rajput 2016), and (3) artificially or traumatically induced radial sieve elements (Sharma *et al.* 1980; Aloni & Barnett 1996). Recently, we found radial sieve tubes in the rays of the secondary xylem in *Aquilaria malaccensis*, *A. sinensis*, *A. crasna* and *Gyrinops versteeghii* (Thymelaeaceae, Malvales). The present study describes the occurrence and structure of radial sieve tubes, in these four well-known agarwood species.

## MATERIALS AND METHODS

The materials studied came from different species, provenances, and stem diameters (see Table 1).

All samples were immediately fixed in 4% formaldehyde. Transverse, radial and tangential sections of 6–8  $\mu\text{m}$  thickness, from different internodes embedded in paraffin, were obtained using a rotary microtome (Leica RM2145). Meanwhile, cross, radial and tangential sections of 15–25  $\mu\text{m}$  thickness were obtained from small shoots and blocks embedded in polyethylene glycol (PEG) 1500 using a sliding microtome (Yamato-Koki Co Ltd, TU-213). For fluorescence microscopy, sections were stained with 0.005% (weight/volume) aniline blue in 0.15 M  $\text{K}_2\text{HPO}_4$  at pH 8.2 for 30 min at room temperature (Currier & Strugger 1956). For double staining, sections were stained with 0.5% safranin for 4 hours followed by 1-minute 0.5% fast green staining, or with compound dye including 1.0% safranin and

Table 1.  
A list of agarwood specimens used in this study.

Specimen No.	Material	
	Stem diameter	Species, age and provenance
I	1st to 15th internodes	Collected from the main stem of a 10-year old tree of <i>Aquilaria sinensis</i> cultivated in the greenhouse of Southwest Forestry University, Kunming, P.R. China.
II	3 cm diameter branch	Collected from the main stem of a 10-year old tree of <i>A. sinensis</i> cultivated in the plantation of Guangdong, P.R. China.
III	Wood blocks	Used in our previous studies (Luo et al. 2018) and collected from the main stem of a 10-year old tree of <i>A. sinensis</i> cultivated in the same plantation as II.
IV	1st to 10th internodes	Collected from a branch and stem of 6-year old trees of <i>G. versteeghii</i> , growing in the plantation of Lombok island, Indonesia.
V	1.2 cm diameter branch	Collected from the same tree described in IV.
VI	Wood blocks	Collected at breast height from the main stem of <i>A. crasna</i> , <i>A. microcarpa</i> and <i>A. malaccensis</i> planted in an agarwood plantation in Pekanbaru, Indonesia.

0.5% astra blue for 4 hours. Some of the aniline blue-stained sections with marked sieve tubes used for fluorescence microscopy were washed and dehydrated by the normal procedure prior to freeze-drying. After freeze-drying, the sections were coated with platinum at 30 mA for 90 s by means of an Ion Sputtering Apparatus (JEOL JEC-3000FC) and examined by field emission scanning electron microscope (FE-SEM) (JEOL JSM-7800F) at 2.0 kV accelerating voltage with a 9–10 mm working distance.

For calculation of the number of radial sieve tube strands and interxylary phloem in secondary xylem, serial cross sections were made from material (V). For counting the number of sieve tubes, preliminary testing was carried out, indicating that aniline blue staining coupled with fluorescence microscopy gave the best results. Therefore, twenty-five serial sections were stained with aniline blue and the number of radial sieve tube strands was counted using fluorescence microscopic pictures. After this step, all slides were washed with deionized water and double-stained with a mixture of safranin and astra blue. Then, the cross-sectional images were photographed with a stereoscopic microscope (Wild M3Z) and the whole area of the secondary xylem in individual sections was measured with image J. Furthermore, the number of interxylary phloem was counted directly on the printed figures of transverse sections.

## RESULTS

Figure 1 shows a typical transverse sectional image of the 14th internode in *A. sinensis*. Approximately, four layers of IP are embedded in the secondary xylem (long double-headed

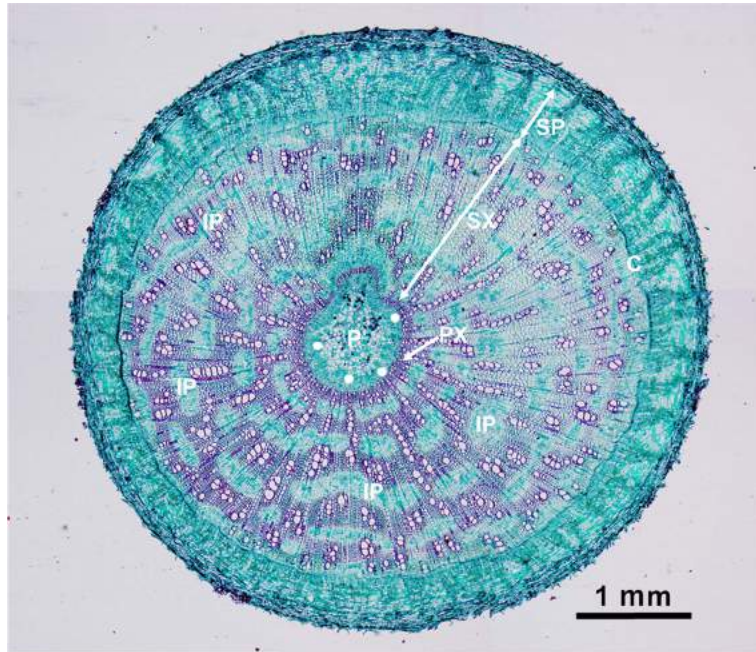


Figure 1. Transverse section (TS) of fourteenth internode in *Aquilaria sinensis*, showing general anatomy of the stem. C = cambium; IP = interxylary phloem; P = pith; PX = primary xylem; SX = secondary xylem; SP = secondary phloem; white dots = intraxylary phloem.

arrow in Fig. 1) which is surrounded by the secondary phloem (short double-headed arrow), being interrupted by the cambium. Primary xylem (arrow) and intraxylary phloem (white dots) are located inside, between secondary xylem and pith. The size and distribution of IP strands in the two genera does not show any differences. The presence of IP strands with a tangential width wider than 400  $\mu\text{m}$  and an axial length longer than 10 mm was very common in *G. versteeghii*. It was also common that one to fifteen rays passed through individual IP strands depending on their tangential widths. The structure and development of intraxylary phloem in both genera is similar to our earlier observations on *A. sinensis* (Luo *et al.* 2019). Furthermore, not only the location and developmental sequences of IP strands, but also the occurrence and structural characteristics of radial sieve tubes are also similar in both genera.

#### *Occurrence and structure of radial sieve tubes in Aquilaria and Gyrinops*

The differentiation of secondary xylem and IP in *A. sinensis* and *G. versteeghii* initiated in the second and third internode respectively. Development of radial sieve tubes was delayed compared to the axial ones located in IP in these two species. Radial sieve tubes were rarely observed in serial cross sections obtained from the third, sixth, and eleventh internodes of *A. sinensis*; however, one radial sieve tube strand was found in a transverse section of the fifteenth internode of *Aquilaria*. Occasionally, radial sieve tubes in *Gyrinops* were observed



in the secondary xylem close to the pith (dotted ellipse in Fig. 2a). Radial section of a 6th internode of *G. versteeghii* revealed a radial sieve tube that initiated differentiation in the cambial zone (Fig. 2b). The figure shows two sieve plates that exhibit fluorescence in the end wall of a radial sieve element (dotted ellipse).

#### *Structural features of radial sieve tubes*

Radial sieve tubes were detected as several bright dots by callose staining on sieve plates in *Aquilaria* and *Gyrinops*. These radial sieve tubes were found in uniseriate as well as in multiseriate rays embedded in secondary xylem and they served as a bridge between two IP strands (Fig. 2c). The radial sieve tubes in an uniseriate ray were similar, or slightly shorter in length, than the ray parenchyma cells. Uniseriate rays that included a sieve tube were slightly wider than the others (Fig. 3a). Multiseriate rays in *Aquilaria* and *Gyrinops* sometimes showed a group of 2–4 sieve tube elements that occurred side-by-side in parallel rows. Most of these sieve tubes had a slender cytoplasmic body and showed more or less twisted or bent shape. Radial sieve tubes are commonly associated with 1–2 companion cells and form a functional unit similar to the axial sieve tubes in IP strands. Sieve plates (and sieve areas) in radial sieve tubes were observed not only at their end wall, but also at their lateral walls similar to axial sieve tubes in *Aquilaria* and *Gyrinops*. Figure 4a shows three spots of bright fluorescence in the lateral (horizontal) wall of a radial sieve tube (arrows in white circle). Generally, radial sieve tubes form one to four or more parallel strands. Figure 4a shows four radial sieve tubes in a single ray. Sieve plates with dense contour and open pores (suggesting doughnut-like deposits) in *A. malaccensis* provides direct evidence that the cell coincides with a radial sieve tube embedded in the marginal or body ray cells (Fig. 3b).

#### *Frequency of radial sieve tubes in the secondary xylem*

The radial sieve tube strands in cross sections were observed at a relatively low frequency compared to that of interxylary phloem strands in all sections examined in this study. The frequency of radial sieve tubes and IP strands was investigated in branch wood with 1.2 cm diameter of *G. versteeghii*, which already produced a large amount of IP. The number of radial sieve tube strands were counted from 25 serial cross sections stained by aniline blue and the number of IP was counted from 10 cross sections. Further, the area occupied by secondary xylem was measured in transverse section after staining with compound dye of safranin and astra blue. Table 2 shows the results of our measurements. The total surface area measured in 25 transverse sections was 2811.9 mm<sup>2</sup>. The total number of radial sieve tubes was found to be 97, irrespective of their length. The average number of radial sieve tubes per mm<sup>2</sup> was 0.034. Fifty of 20 µm-thick sections can be cut in 1 mm-thick secondary xylem. Therefore, 1.7 radial sieve tubes is calculated per mm<sup>3</sup>. On the other hand, total number of IP was 11 050 in total area of 1214.7 mm<sup>2</sup>. The average number of interxylary phloem was calculated as 9.1 per mm<sup>2</sup>.

#### *Structural characteristics of minute sieve pores in radial sieve tubes*

Scattered minute sieve pores independent from the sieve plate were observed in all radial sieve tubes. These pores were stained by aniline blue, evidencing that they are surrounded by a callose collar. Many such sieve pores were distributed randomly or in clusters (sieve area) on the horizontal/lateral wall of radial sieve tubes, as shown in Figure 4b. The

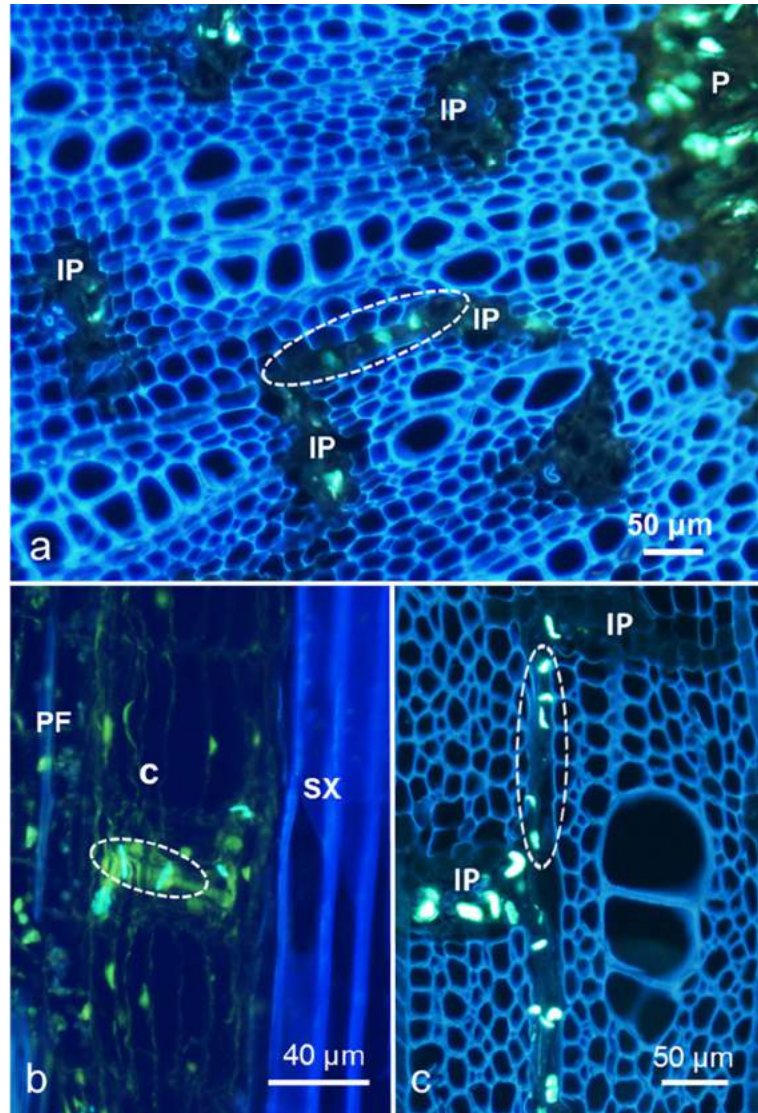


Figure 2. Fluorescence microscopy image taken after aniline blue staining. (a) TS of 1.2 cm-diameter branch wood of *Gyrynops versteeghii* shows the occurrence of a radial sieve tube (dotted ellipse) bridging two IPs close to the pith. IP = interxylary phloem; P = pith. (b) Radial section (RS) in 6th internode of *G. versteeghii* shows a differentiating radial sieve tube strand (dotted ellipse) in the cambium. C = cambium; SX = secondary xylem; PF = secondary phloem fiber. (c) TS shows a radial sieve tube bridging over two IPs in a 3-cm-diameter branch of *Aquilaria sinensis*. IP = interxylary phloem.

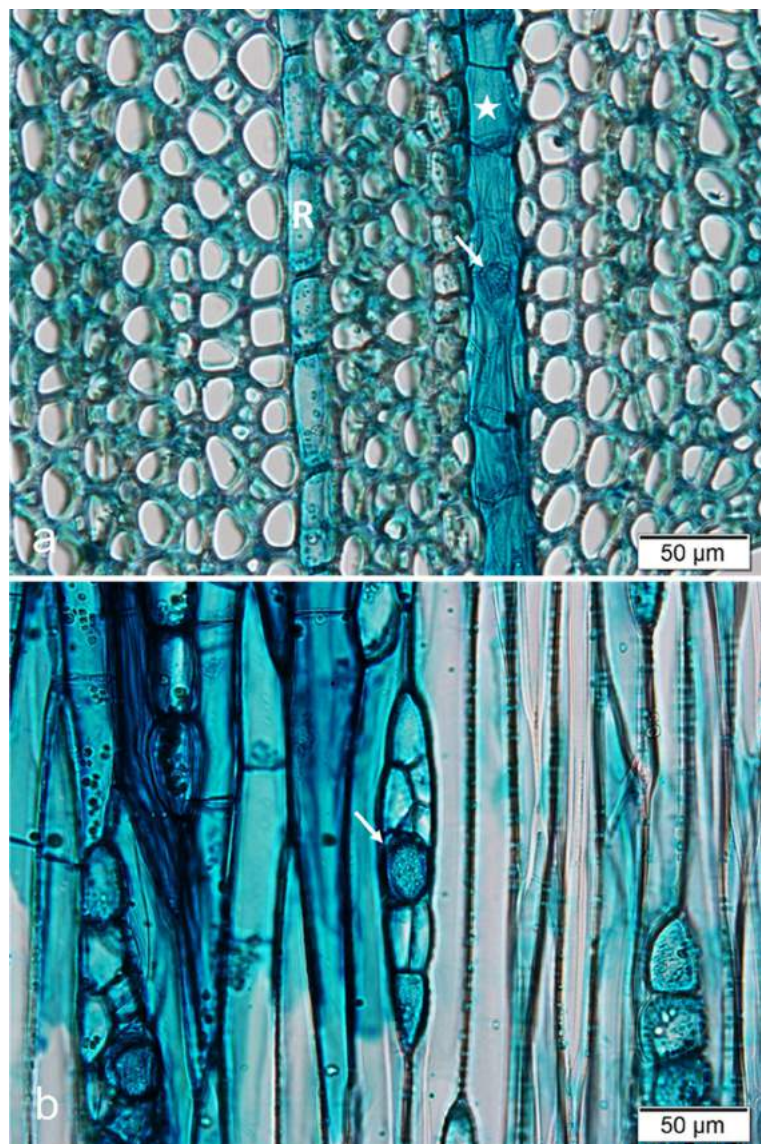


Figure 3. (a) TS of secondary xylem in *A. malaccensis* shows a radial sieve tube strand (asterisk) which is wider than the normal uniseriate ray (R). The arrow indicates a sieve plate of a radial sieve tube strand. (b) Tangential section of the secondary xylem in *A. malaccensis* shows a cross face of a radial sieve tube strand with dense marginal contour in the center of a ray tissue (arrow).

size of the sieve pores, including the collar, was approximately 0.5–0.8  $\mu\text{m}$ , with the size of pore itself being less than 0.1  $\mu\text{m}$ . The distribution of the minute sieve pores was irregular, but they were localized in some limited areas. Therefore, many parts of cell wall in radial sieve tubes did not show any sign of such pores.

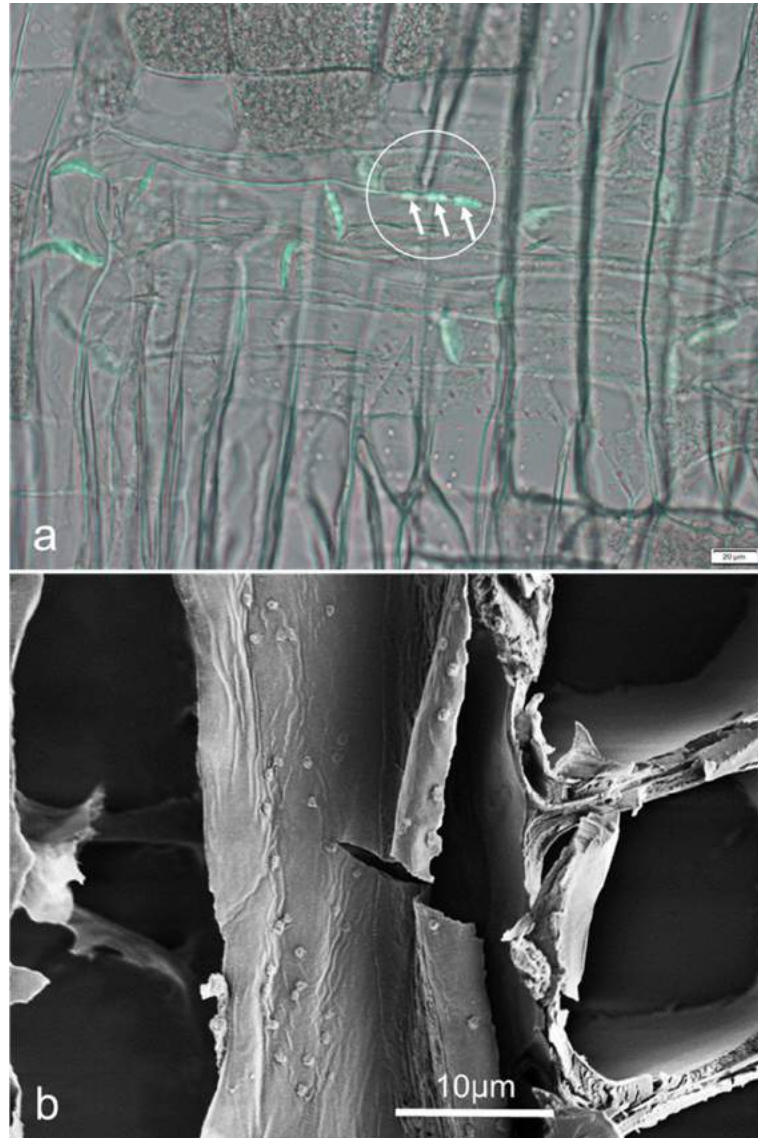


Figure 4. (a) RS of secondary xylem of *A. sinensis* viewed by a combination of bright field and fluorescence light showing sieve plates (circle) in the lateral wall of one of four radial sieve tube strands. Arrows show sieve plates. Scale bar = 20  $\mu\text{m}$ . (b) FE-SEM image of a radial sieve tube in a 3 cm-diameter branch of *A. sinensis*, showing many scattered minute sieve pores in the inner surface of the horizontal/lateral wall.

Table 2.  
The number of ray sieve tubes and IP per unit area of secondary xylem.

Serial section	Secondary xylem area (mm <sup>2</sup> )	No. of radial sieve tubes	No. of interxylary phloem (IP)
1	121.4	4	–
2*	121.3	3	1113
3*	121.3	1	1113
4*	117.5	0	1105
5*	122.9	2	–
6*	120.1	5	1095
7*	125.1	3	1102
8*	119.2	6	–
9*	124.2	6	–
10*	120.2	6	–
11*	121.3	3	–
12*	121.3	7	1109
13*	121.3	5	1084
14*	121.3	5	1114
15*	121.3	6	1107
16	108.7	4	–
17	91.7	0	–
18	83.5	4	–
19	108.4	1	–
20	102.1	3	–
21	84.9	6	–
22	90.9	4	–
23	11.7	6	–
24	108.4	2	–
25	101.9	5	–
Total	2811.9	97	11 050

–, No measurement of IP number.

\*Complete section without defects in the secondary xylem.

### ***Connection between radial and axial sieve tubes***

Connection between radial and axial sieve tubes is a common feature in all species of *Aquilaria* and *Gyrinops* that were investigated. An integrated radial sieve tube strand that is not interrupted by other cells or tissues usually consists of one to several sieve elements. Most of the sieve tubes in the middle part of the strand run parallel to ray parenchyma cells, while sieve tubes at the opposite ends of strand sometimes exhibit a sharp angle. Various types of connections having different angles and directions were observed between radial and axial sieve tubes.

### ***Connection by bending of radial sieve tube strands***

The successive connections between radial sieve tubes in rays and axial IP sieve tubes can be observed in Fig. 5a. Because of their interaction with axial sieve tubes, most radial

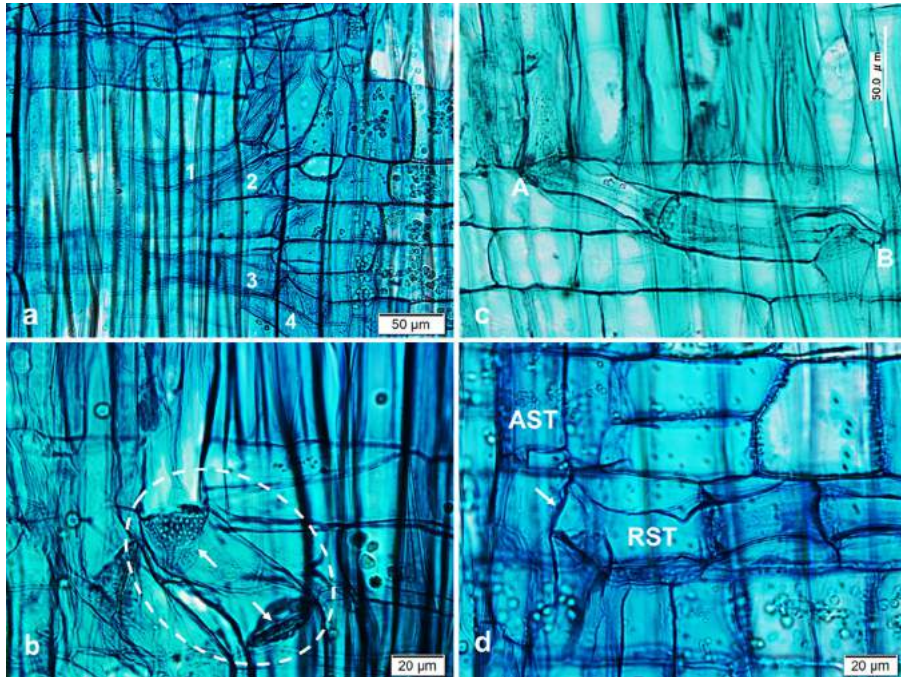


Figure 5. RS of secondary xylem in *A. malaccensis*. (a) Four radial sieve tube strands (1 to 4) that are bending vertically. (b) S-shaped connection (dotted ellipse) of radial sieve tube strand. Arrows show sieve plate. (c) L-shaped connection between radial and axial sieve tubes on both sides (A and B). (d) T-shaped connection between radial and axial sieve tubes. A radial sieve tube strand has a connection with an axial sieve tube through a common sieve plate (arrow). AST, axial sieve tube; RST, radial sieve tube.

sieve tubes more or less deviated from a horizontal direction and exhibited a sharp angle with ray parenchyma cells, especially cells located at the end of a sieve tube strand. In Fig. 5a, four radial sieve tubes (1 to 4) within a ray tissue were bent towards a vertical direction, giving the impression of curved channels.

#### *Connection of two strands by an oblique bridge*

In some cases, the radial section of *A. malaccensis* displayed a very steeply curved sieve tube. Each end of an oblique sieve element was connected to an axial sieve tube, thus forming an S shape connection (Fig. 5b). A sieve tube oriented in radial and tangential direction just like an oblique bridge within IP (dotted circle in Fig. 6) was observed in the transverse section. Both ends of the sieve tube may connect with axial sieve tubes through the junction of sieve plates (arrows). An oblique bridge was not a common feature, but it was observed in some cases.

#### *Connection of two strands at a right angle*

*L-shaped connection.* Figure 5c shows two connecting parts at the opposite ends of one radial sieve tube strand that are composed of only two elements in *A. malaccensis*. Sieve

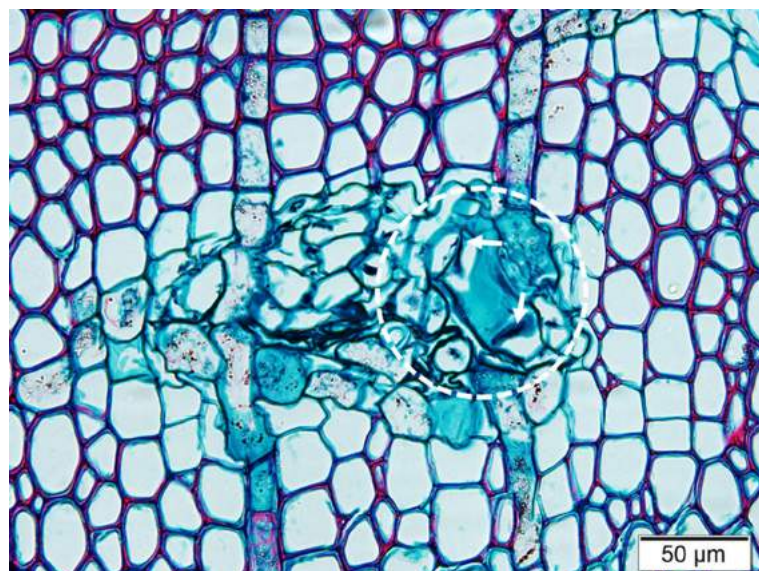


Figure 6. TS of secondary xylem in *A. sinensis* showing oblique bridge of a radial sieve tube (dotted circle) with possibly two axial ones. Arrows show sieve plate.

plates of radial sieve tube elements are attached with cytoplasmic material connecting to axial sieve tubes in both ends separately. The left end of the radial sieve tube strand shows a distinct connection with an axial sieve tube strand, just like an L-shaped connection (A in Fig. 5c). The junction on the right end of the radial sieve tube is located in its lateral wall where an axial sieve tube is connected at right angle (B in Fig. 5c).

*T-shaped connection.* Lateral sieve plates constitute another alternative connection between radial and axial sieve tubes. Figure 5d shows a T-shaped connection by a common sieve plate (an arrow) between an axial sieve tube strand on the left and a radial sieve tube strand on the right of *A. malaccensis*.

## DISCUSSION

This study sheds light on the occurrence and structural characteristics of the connection between radial sieve tubes in ray tissue and axial sieve tubes in the interxylary phloem of *Aquilaria* and *Gyrinops* (Thymelaeaceae, Malvales).

### *Occurrence and structure of radial sieve tubes*

Ray tissue generally consists of parenchyma cells, but other elements such as tracheids, vessels, resin ducts and sieve elements also can be found in rays of various species (Lev-Yadun & Aloni 1995; Angyalossy et al. 2016). Occurrence of sieve tube elements in ray tissues is a rare feature.

Our observations confirm the existence of sieve tubes in rays in three species of *Aquilaria* and one species of *Gyrinops* (Thymelaeaceae). These two genera are commonly

characterized by the development of IP in secondary xylem. When radial sieve tubes are observed, most of them have a connection with the IP strands. Interxylary phloem in *Aquilaria* and *Gyrinops* usually starts to develop in the lower part of the third internode in young shoots and grows to about four to five layers in the fourteenth internode. The earliest radial sieve tube strand is observed in the secondary xylem adjacent to the pith, immediately following the differentiation of the first-formed IP. Earlier, we have shown that the first-formed IP strands develop in the third or fourth internode (Luo *et al.* 2018). Additionally, we observe few or dim fluorescence dots in immature IP close to the cambium, indicating that sieve tubes in immature IP strands are not yet fully developed. In the same section, an immature radial sieve tube with sieve plates was observed passing through the cambial zone. Similar results were obtained by Den Outer & Van Veenendaal (1981), who find the existence of radial sieve tubes and companion cells in very wide aggregate rays of *Azima tetracantha* (Salvadoraceae). However, these authors do not confirm the direct connection between axial and radial sieve tubes. Unlike *Azima*, *Aquilaria* and *Gyrinops* generally produce uniseriate as well as multiseriate rays including solitary and/or multiple radial sieve tube strands.

Lev-Yadun & Aloni (1991) suggested a new type of xylem ray with many “ray centers” in *Suaeda monoica* (Amaranthaceae). In some huge rays, radial strands of phloem are observed, and the number of phloem strands increase with the enlargement of the xylem ray in the centrifugal direction. Compared with the multicentric distribution of sieve tubes in huge aggregated ray of *Suaeda monoica*, tangential sections of all the studied samples of *Aquilaria* and *Gyrinops* show radial sieve tubes mostly as a solitary cell or in small groups like those found in the five tropical species reported by Rajput (2004). Radial sieve tubes generally develop from the margin as well as the center of the rays, and they are observed in contact with axial sieve tubes. Our observations of radial sieve tube elements in secondary xylem are consistent with those of Rajput (2004) on secondary phloem.

Independent from the sieve pores constituting sieve plates, the occurrence of scattered and minute sieve pores or their clusters in the lateral wall of radial sieve tube strands in both *Aquilaria* and *Gyrinops* shows the following structural features: clustered sieve pores surrounded by callose deposits and lined up in a direction parallel to the cytoplasmic flow in the radial sieve tube strand. The location of minute sieve pores in the horizontal rather than radial lateral walls in the radial sieve tubes, suggests a more effective transport pathway between the sieve tube and ray parenchyma cells, especially in the case of *Aquilaria* and *Gyrinops* that produce uniseriate or biseriate rays. Metabolite transport may occur through the minute sieve pores as an alternative to pore-plasmodesmata units described by Cayla *et al.* (2015).

After measuring the area of secondary xylem in *G. versteeghii* and counting the number of radial sieve tube strands, it is found that a complete cross section includes only four radial sieve tube strands on average (Table 2). Compared to the occurrence of a great number of IP that include more than one axial sieve tube strands per IP, the number of radial sieve tubes present in a cross section seems almost negligible for serving the translocation of photosynthates. It is suggested that radial sieve tubes may be temporarily involved in short-distance rapid transport of food nutrients under stress derived from injuries or other



environmental changes, as has been discussed in the case of radial sieve tubes in the secondary phloem of five tropical tree species (Rajput & Rao 1997; Rajput 2004). However, it is meaningful to recall the long axial length of IP. For instance, the average length of IP in *A. sinensis* is  $14 \pm 4$  mm according to our former paper (Luo *et al.* 2018) and IP longer than 10 mm is very common in *G. versteeghii*. The significant number of radial sieve tubes and interxylary phloem, that is, 1.7 per  $\text{mm}^3$  and 9.1 per  $\text{mm}^2$  present enough to connect each other in the secondary xylem. Further, the number of radial sieve tubes will potentially increase with the increase in thickness of the secondary xylem, which suggest a considerable number of connection between axial and radial sieve tubes. Considering the fact that IP strands are completely isolated from each other in the secondary xylem and none of the axial sieve tubes have direct contact, the presence of direct connections between radial sieve tubes in the ray tissue and axial sieve tubes in IP strands could play a significant role in the translocation of metabolites.

#### **Connection between radial and axial sieve tubes**

The connections between radial and axial sieve tubes shown in the present work are an integral part of phloem anastomosis in *Aquilaria* and *Gyrinops*. In general, phloem anastomosis is very common in higher plants for the aim of fast and alternative communication (Aloni *et al.* 1990, 1995). In *Cucurbita dahlia* (Cucurbitaceae), the earliest signs of phloem anastomosis begin to be detected from the internode with a length of about 5 mm (Aloni & Barnett 1996). Similar anastomosis of sieve tubes is a common feature in different internodes of *Coleus* (Lamiaceae) (Aloni *et al.* 1990). In addition to the naturally developing structures, phloem anastomoses composed of a large number of sieve tubes are reported in stems of *Ricinus communis* (Euphorbiaceae) infected by *Agrobacterium tumefaciens* (Aloni *et al.* 1995).

The first sign of radial sieve tubes is observed immediately after the formation of the first layer of IP in the secondary xylem at the 15th internode. Distinctive aniline-blue staining of radial sieve tubes in *G. versteeghii* appear in the cambial zone cells in the 6th internode. Once radial sieve tubes are produced, they could have a connection with axial sieve tubes in one or two IP strands. These observations suggest that the network formation of phloem anastomosis depends on the activity of vascular cambium. With the continued differentiation of interxylary phloem, the number of radial sieve tubes increases with increase in the stem diameter. As a result, all sieve tubes within the plant might gradually establish a collective sieve tube system (Ham & Lucas 2014).

Radial transfer of water from phloem to xylem via ray parenchyma cells is confirmed by fluorescence dye injection (Pfausch *et al.* 2015). The necessity of sieve tube differentiation in ray system comes from the need for selective transport and intercellular communication via elaborate channels in sieve plate (Amsbury *et al.* 2018). It is suggested that development of radial sieve tubes in the ray system will help shorten the distance for transport of nutrients (Rajput & Rao 1997; Rajput 2004). Four or more strands of radial sieve tubes found in *A. malaccensis* may suggest that radial phloem is capable of shortening the transport of photosynthates.

Finally, what is the source of radial sieve tube strands in the secondary xylem? There are two possibilities for the origin of radial sieve tube strands – one from re-differentiation of ray parenchyma cells, and the other from the division and differentiation of vascular cambium similar to the origin of vessels, ray parenchyma and xylem fibers. As discussed earlier, various types of connections between radial and axial sieve tubes are found in the three species of *Aquilaria* and one species of *Gyrinops* analyzed in this study. These connections occur in vertical, horizontal and radial directions and can be easily formed during the differentiation of cambium. Considering the occurrence and development of these different types of connections of radial sieve tube strands, it is not realistic to imagine that radial sieve tubes are produced by the re-differentiation of ray parenchyma cells. As shown in Fig. 2b, radial sieve tubes differentiate in the cambial zone, and are thus originated from cambium.

#### ACKNOWLEDGEMENTS

This research was conducted mainly at the Research Institute for Sustainable Humansphere, Kyoto University, Japan and was supported by the National Natural Science Foundation of China (CN) (Grant No. 31700481). Part of the experiments were performed at University Gadjah Mada, Yogyakarta, Indonesia and University Mataram, Mataram, Indonesia. Part of the experimental materials (shoots of *Aquilaria sinensis*) was obtained through a grant by the National Natural Science Foundation of China (CN) (Grant No. 31570555). The author wishes to thank Ms. Zuoming Tang for her help with microtome sectioning of *Gyrinops versteeghii*.

#### REFERENCES

- Aloni R, Baum SF, Peterson CA. 1990. The role of cytokinin in sieve tube regeneration and callose production in wounded coleus internodes. *Plant Physiol* 93: 982–989.
- Aloni R, Pradel KS, Ullrich CI. 1995. The three-dimensional structure of vascular tissues in *Agrobacterium tumefaciens*-induced crown galls and in the host stems of *Ricinus communis* L. *Planta* 196: 597–605.
- Aloni R, Barnett JR. 1996. The development of phloem anastomoses between vascular bundles and their role in xylem regeneration after wounding in Cucurbita and Dahlia. *Planta* 198: 595–603.
- Amsbury S, Kirk P, Benitez-Alfonso Y. 2018. Emerging models on the regulation of intercellular transport by plasmodesmata-associated callose. *Journal of Experimental Botany* 69(1): 105–115. DOI: 10.1093/jxb/erx337.
- Angyalossy V, Angeles G, Pace MR, Lima AC, Dias-Leme C, Lohmann LG, Madero-Vega C. 2012. An overview of the anatomy, development and evolution of the vascular system of lianas. *Plant Ecology & Diversity* 5(2): 167–182. DOI: 10.1080/17550874.2011.615574.
- Angyalossy V, Pace MR, Evert RF, Marcati CR, Oskolski AA, Terrazas T, Kotina E, Lens F, Mazzoni-Viveiros SC, Angeles G, Machado SR, Crivellaro A, Rao KS, Junikka L, Nikolaeva N, Baas P. 2016. IAWA list of microscopic bark features. *IAWA J.* 37(4): 532–542, 554–555. DOI: 10.1163/22941932-20160151.
- Carlquist S. 2010. Caryophyllales: a key group for understanding wood anatomy character states and their evolution. *Botanical J the Linnean Society* 164: 342–393. DOI: 10.1111/j.1095-8339.2010.01095.x.
- Carlquist S. 2013. Interxylary phloem: diversity and functions. *Brittonia* 65(4): 477–495. DOI: 10.1007/s12228-012-9298-1.

- Cayla T, Batailler B, Le Hir R, Revers F, Anstead JA, Thompson GA, Grandjean O, Dinant S. 2015. Live imaging of companion cells and sieve elements in *Arabidopsis* leaves. *PLoS One* 10(2):1–22. DOI: 10.1371/journal.pone.0118122.
- Chalk L, Chanaway MM. 1937. Identification of woods with interxylary phloem. *Systematic Botany Trop Woods* 50: 1–31.
- Chavan RR, Shah JJ, Patel KR. 1983. Isolated sieve tube (s)/elements in the barks of some angiosperms. *IAWA Bulletin n.s.* 4(4): 255–263.
- Currier HB, Strugger S. 1956. Aniline blue and fluorescence microscopy of callose in bulb scales of *Allium cepa* L. *Protoplasma* 45: 552–559.
- Den Outer RW, van Veenendaal WLH. 1981. Wood and bark anatomy of *Azima tetracantha* Lam. (Salvadoraceae). *Acta Bot. Neerl.* 30: 199–207.
- Den Outer RW, van Veenendaal WLH. 1995. Development of included phloem in the stem of *Combretum nigricans* (Combretaceae). *IAWA J* 16: 151–158.
- Evert RF. 2006. *Esau's plant anatomy*, 3rd Edn. John Wiley & Sons, Inc.
- Gondaliya AD, Rajput KS. 2016. Stem anatomy and development of inter- and intraxylary phloem in *Leptadenia pyrotechnica* (Forssk.) Decne. (Asclepiadaceae). *Plant Biosystems* 151: 855–865. DOI: 10.1080/11263504.2016.1218968.
- Holtta T, Mencuccini M, Nikinmaa E. 2009. Linking phloem function to structure: analysis with a coupled xylem-phloem transport model. *Journal of Theoretical Biology* 259: 325–337. DOI: 10.1016/j.jtbi.2009.03.039.
- Lev-Yadun S, Aloni R. 1991. Polycentric vascular rays in *Suaeda monoica* and the control of ray initiation and spacing. *Trees* 5: 22–29.
- Lev-Yadun S, Aloni R. 1995. Differentiation of ray system in woody plants. *The Botanical Review* 61(1): 45–84.
- Luo B, Ou Y, Pan B, Qiu J, Itoh T. 2018. Structure and development of interxylary and external phloem in *Aquilaria sinensis*. *IAWA J.* 39: 3–17. DOI: 10.1163/22941932-20170182.
- Luo B, Imai T, Sugiyama J, Qiu J. 2019. The occurrence and development of intraxylary phloem in young *Aquilaria sinensis* shoots. *IAWA J.* 40: 23–42. DOI: 10.1163/22941932-40190221.
- Mohamed R, Wong MT, Halis R. 2013. Microscopic observation of 'Gaharu' wood from *Aquilaria malaccensis*. *Pertanika J. Trop. Agricult. Sci.* 36: 43–50.
- Patil VS, Marcati CR, Kishore KS. 2011. Development of intra- and interxylary secondary phloem in *Coccinia indica* (Cucurbitaceae). *IAWA J.* 32: 475–491. DOI: 10.1163/22941932-90000072.
- Patil VS, Rajput KS. 2008. Structure and development of inter- and intraxylary phloem in *Leptadenia reticulata* (Asclepiadaceae). *Polish Botanical J.* 53: 5–13.
- Pfautsch S, Renard J, Tjoelker MG, Salih A. 2015. Phloem as capacitor: radial transfer of water into xylem of tree stems occurs via symplastic transport in ray parenchyma. *Plant Physiology* 167: 963–971. DOI: 10.1104/pp.114.254581.
- Rajput KS, Rao KS. 1997. Occurrence of sieve elements in phloem rays. *IAWA Journal* 18(2): 197–201.
- Rajput KS. 2004. Occurrence of radial sieve elements in the secondary phloem rays of some tropical species. *Israel Journal of Plant Sciences* 52: 109–114.
- Rajput KS, Patil VS, Rao KS. 2009. Development of included phloem of *Calycopteris floribunda* Lamk. (Combretaceae). *The Journal of the Torrey Botanical Society* 136: 302–312. DOI: 10.3159/09-RA-010.1.
- Rajput KS, Patil VS, Rao KS. 2013. Wood anatomy and development of interxylary phloem of *Ipomoea hederifolia* Linn. (Convolvulaceae). *J. Plant Growth Regul.* 32: 654–662. DOI: 10.1007/s00344-013-9334-8.
- Sharma HK, Sharma DD, Paliwal GS. 1980. Induction of sieve tube elements in the ray system of *Morus alba* L. *Biologie Plantarum* 22: 152–153.

Van Veenendaal WLH, den Outer RW. 1993. Development of included phloem and organization of the phloem network in the stem of *Strychnos millepunctata* (Loganiaceae). *IAWA Journal* 14(3): 253–265.